Science Arts & Métiers (SAM)

is an open access repository that collects the work of Arts et Métiers Institute of Technology researchers and makes it freely available over the web where possible.

This is an author-deposited version published in: https://sam.ensam.eu
Handle ID: .http://hdl.handle.net/10985/23584

To cite this version :

Yunho AHN, Guido ROMA, Xavier COLIN - Elucidating the Role of Alkoxy Radicals in Polyethylene Radio-Oxidation Kinetics - Macromolecules - Vol. 55, n°19, p.8676-8684 - 2022

Any correspondence concerning this service should be sent to the repository Administrator : scienceouverte@ensam.eu

Arts et Métiers Institute of Technology

Elucidating the Role of Alkoxy Radicals in Polyethylene Radio-Oxidation Kinetics

Yunho Ahn, Guido Roma,* and Xavier Colin

ABSTRACT: Polyethylene is a widely used polymer and a prototypical polyolefin. Understanding degradation mechanisms at the atomic scale leading to oxidation under the effect of temperature and/or irradiation is crucial for many long-term applications. Here, we focus on a subset of reactions belonging to the generally assumed radio-oxidation reaction scheme and involving alkoxy radicals. We follow a theoretical approach based on density functional theory, in order to assess the role of these species, which are short lived and thus hard to detect experimentally. For every considered reaction, we calculate the reaction enthalpy and the energy barrier, and we evaluate the influence of the local atomic environment, taking advantage of a model surface of a crystalline lamella which mimics the interface between crystalline and amorphous zones. Our results suggest that in certain conditions, the kinetic pathway can bypass the formation of hydroperoxides. The concentrations of alkoxy and peroxy radicals during radio-oxidation and their ratio are important parameters controlling the predominance of chain scission or crosslinking in the polymer. The data presented here constitute part of a database that can be used to set up kinetic simulations based on homogeneous chemical kinetics or Monte Carlo algorithms.

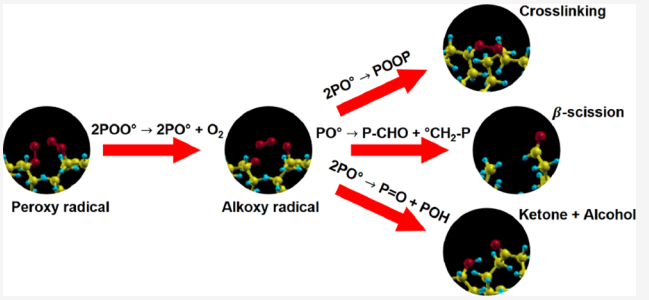

INTRODUCTION

Degradation of polymers is a complex phenomenon involving not only environmental parameters like humidity, oxygen partial pressure, and temperature but also irradiation by light or other emission sources. The application domains where a better predictability of polymer lifetime would be welcome are various. One of them is for electrical insulation, for example, to ensure reliable operation of electrical cables in nuclear power plant (NPP) reactor buildings.[1] In operating conditions, oxidation is the main degradation process occurring in cable insulators made of polyethylene (PE). Under high temperature and/or irradiation (typically γ-rays in NPPs but could also be UV, electrons, and swift heavy ions in different environments), alkyl radicals are generated and react with oxygen by forming peroxy radicals. This process leads to other oxidative radical species or byproducts, causing severe chemical and/or mechanical degradation. This is the first ingredient of the basic autooxidation scheme (BAS), developed by Bolland and Gee,[2] which was soon widely applied to various types of polymeric materials[3,4] and still is today,[5−7] with some variants/improvements. Assuming the production of alkyl radicals, essentially by decay of highly excited electron states on timescales much shorter than diffusion or chemical reactions, the production of peroxy radicals is essentially limited by diffusion of oxygen molecules in the material; diffusion is generally assumed to occur essentially in the amorphous phase,[8] and the barrierless formation of peroxy radicals is well established.[9,10]

The following step of the BAS is the formation of hydroperoxides which have since long time been shown to be a relevant transient species, reaching a stationary concentration;[3] the activation energy for this reaction was estimated both experimentally[6] and theoretically[10] to be around 0.7 eV, but its relevance was recently questioned due to a positive reaction enthalpy[7,11] which is close to the activation energy itself, making the POOH species coming from this reaction quite short lived. Up to now, the possibility that the energy release stemming from the formation of peroxides from O_2 capture leads to direct formation of hydroperoxides, which could be investigated through dynamical simulations, has not been considered.

Assuming nevertheless that hydroperoxide species, including those initially present in the polymer,[12] are available, according to the BAS scheme, they should be decomposed following two main reaction pathways—as chain branching steps—by forming radical species: (i) an alkoxy radical and a hydroxyl radical (POOH → $PO^{\bullet}$ + $^{\bullet}OH$) (unimolecular reaction) and (ii) a peroxy radical, an alkoxy radical, and a water molecule (2POOH

→ $POO^{\bullet}$ + $PO^{\bullet}$ + H_2O) (bimolecular reaction). The comparison of the activation energies of these two reactions is of course crucial in order to determine the reaction pathways, depending on the degradation conditions.[13] For the first reaction, various estimations of the activation energy have been proposed, both from experiments[12,14−16] and from theoretical calculations,[9,10,17,18] the former spanning values between 0.7 and 1.6 eV, while the latter, that is, theoretical values, are somewhat higher in the small interval between 1.8 and 2.1 eV, in spite of differing levels of theory. Such relatively high activation energies question the actual role of this mechanism in the degradation process, suggesting that the global scheme should be reconsidered with a closer comparison to other possible reactions, leading to the formation of these radicals.

The relative predominance of these two reactions depends of course strongly on the concentration of hydroperoxide species and/or their diffusion in the reactive medium.

When the alkoxy and hydroxyl radicals are produced by the two mentioned reactions, they affect other propagation reactions (e.g., $POO^{\bullet}$ + P → POOH + $P^{\bullet}$), chain branching (e.g., $PO^{\bullet}$ + PH → POH + $P^{\bullet}$), and/or termination steps (e.g., $POO^{\bullet}$ + $P^{\bullet}$ → POOP).

Furthermore, radical species, in particular alkoxy radicals, are supposed to be involved in various reactions such as cross-linking, chain scission, and the production of carbonyl defects, generally considered the final stage of degradation of PE.

Some of these mechanisms were investigated in a recent paper[19] of which we became aware during the review process. The outcome, for PE, relying on a careful kinetic model based on reaction rates from the literature and from ab initio calculations globally support our conclusions.

Another point that has been rarely addressed is how the various reaction rates are affected by the local environment (crystalline, amorphous, or at the interface between the two). Most theoretical approaches, including the recent paper by De Keer et al.,[19] consider reactions for molecules in the gas phase,[18,20−22] others recently have considered crystalline or surface environments;[9,10] this issue is a relevant one to understand the actual reaction pathways, also because frequently the crystallinity ratio can evolve during the oxidation processes.[23] Given the complex microstructure of PE, featuring crystalline lamellae typically 10 nm thick,[24,25] separated by amorphous regions, the dominant oxidation reaction pathways could be different according to the local environment (i.e., amorphous phase, inside crystalline lamellae, or at their surface). This factor can be taken into account in atomic scale calculations, while it is more difficult to study it experimentally. For example, we show below that the formation of alkoxy radicals takes place very easily (without any barrier) when two peroxy radicals are close to each other at the crystalline lamellae surface. For the other reactions, crosslinking, chain scission, and carbonyl defects are mainly studied; in some cases, not only the global environment but also the involved chains (unimolecular/bimolecular reaction) and even the exact position of the radicals influence the obtained energy barriers.

In this paper, after our previous work focusing on the formation and decomposition of hydroperoxides,[10] we focus on reactions involving alkoxy radicals, in order to compare the activation energies and reaction enthalpies of several reactions on the same footings. We also consider systematically the role of the local environment, setting up three different models for the crystalline, amorphous, and interface regions, to understand where each reaction preferentially occurs.

As in our previous work, our approach is based on density functional theory (DFT) and the nudged elastic band method (NEB)[26] for exploring the energy landscape.

A summary of possible reaction pathways of the oxidation of PE, including the main steps of the BAS, is graphically shown in Figure 1. We selected several main products during the oxidation. First, we investigated the formation of radical species, mainly focusing on alkoxy radicals which could determine the final products such as crosslinking, chain scission, and carbonyl defects. Then, as peroxy radicals from the BAS can also form alkoxy radicals, we investigate their fate, following several possible reaction pathways.

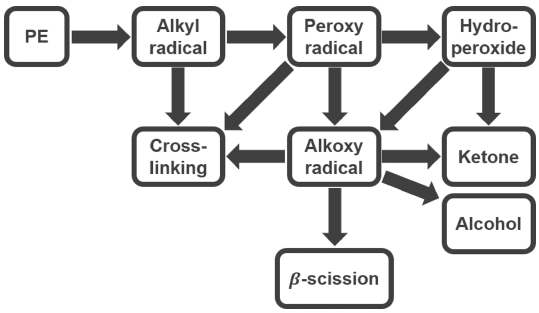

Figure 1. Summary of reaction pathways for the overall oxidation process of PE.

METHODS AND POLYMER MODELS

All the results presented in this paper are based on DFT. Equilibrium structures and their total energies are obtained from the Quantum-Espresso software package[27] (versions 6.5) by using the PWSCF module pw.x. The energy barriers and reaction pathways are calculated by the climbing image NEB[26] method, as implemented in the Quantum-Espresso distribution. Quantum-Espresso is publicly available through the official site [http://quantumespresso.org (accessed on 21 June 2021)]. The NEB method being a static one, we neglect here temperature effects on the free energy barriers as we do not add entropic contributions. The estimation of entropic contributions to reaction barriers, which might be non-negligible especially for reactions with very low or no barrier, should be performed with dynamical methods which are clearly out of the scope of the present paper. We provide further discussion of this issue in the Supporting Information.

We rely on three models, whose graphical representation is provided in the Supporting Information. The first one is based on isolated molecules of varying lengths, and the second one is crystalline PE in the orthorhombic structure, as described in ref 28. We will call them below molecular and crystalline lamellae models, respectively. The third one is called the lamellae surface mimicking the interface between two crystalline regions, with bent polymer chains at the crystal surfaces. We constructed this model in the following way: a slab was cut from a 96 atom supercell of the orthorhombic crystal along planes perpendicular to the polymer chains. The dangling chains were passivated by adding 12 CH_2 units (six on each slab surface) and then relaxed keeping the lattice parameters of the orthorhombic crystal on the slab surface and raising the lattice parameter along the chains, so that the two facing surfaces are separated by approximately 7 Å; although this distance is much smaller than the actual inter-lamellae spacing observed experimentally,[24,25] it is such that the interaction between neighbouring surfaces is negligible. Our surface to volume ratio is of the same order of magnitude (0.7 nm^{-1}) of that estimated from data given in ref 25 (∼0.4 nm^{-1}). While reactions occurring on isolated molecules might well represent unimolecular reactions occurring in the lowest density regions of the amorphous zone, the crystalline lamellae and their surface

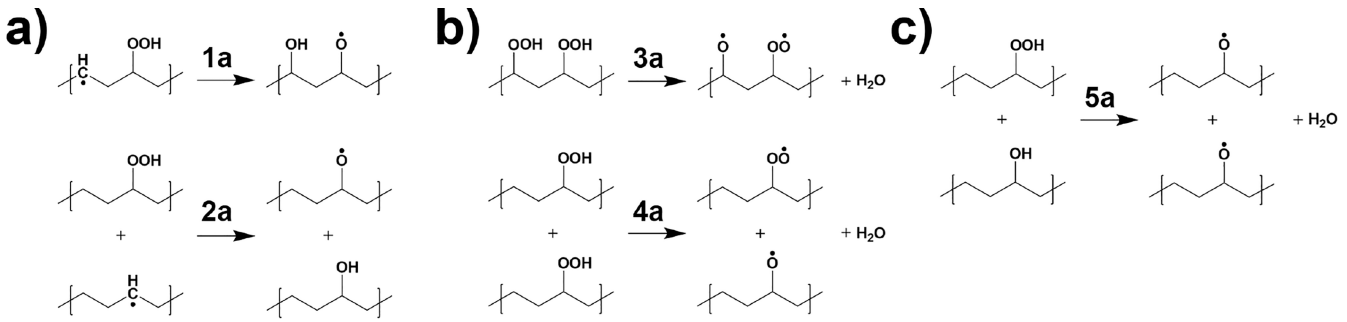

Figure 2. Reaction pathways leading to the production of alkoxy radicals from decomposition of hydroperoxides either through alkyl radicals (a) or by bimolecular conversion (b) or reusing an alcohol (c) produced in reaction 2a.

are able to describe intermolecular (namely, bimolecular) reactions occurring in the crystal and at the crystal/amorphous interface. Moreover, the boundary between the amorphous and the crystalline regions is hardly well defined due to the roughness of lamella surfaces,[25] the peculiar morphology of the samples; furthermore, the region where chains bend is sometimes considered as included in the amorphous zone.[29] For molecular models, we used body-centered tetragonal unit cells in order to maximize the chain end distance between periodic images of the molecules; the unit cells were 40 × 40 bohr wide in the plane perpendicular to the chain, and they exceeded the molecule length in the direction parallel to the chain so as to have at least a distance of 25 bohr between atoms of two different periodic images. The unit cell of the crystalline lamellae is orthorhombic, containing 12 atoms, and we sampled the Brillouin zone with a 3 × 3 × 6 Γ-centered regular *k*-point mesh. To model isolated defects in the solid, we used a 2 × 1 × 4 supercell (containing 96 atoms, plus defects), and we employed a 2 × 3 × 2 Γ-centered *k*-point mesh. The theoretical equilibrium lattice parameters of the orthorhombic unit cell in atomic units were: a = 9.18 bohr, b = 13.14 bohr, and c = 4.84 bohr, and for the 2 × 1 × 4 supercell: a = 18.36 bohr, b = 13.14 bohr, and c = 19.36 bohr. The unit cell of the lamellar surface, containing 132 atoms for pure PE, is similar to a model previously used to describe a carboxyl group grafted onto a lamella.[30] Pseudopotentials, norm-conserving (nc) for C and H and both nc and ultrasoft for oxygen, were generated, as described in ref 28 and used with the optB86b + vdW exchange−correlation (xc) functional.[31] The functional optB86b + vdW includes a gradient-corrected short range xc contribution and a long-range non-local van der Waals correlation term in order to provide a good description of van der Waals interchain interactions in crystalline PE. Our calculations, performed with a plane-wave basis set with a cutoff energy of 60 Ry and *k*-point sampling corresponding to a Γ-centered 3 × 3 × 6 grid in the PE orthorhombic unit cell for the solid and lamellar models, allowed an accuracy on energy differences of a few hundreds of an eV (further information on the accuracy of energy barriers is provided in the Supporting Information).

RESULTS

Formation of Radical Species. As a starting point for our investigation, we note that in contrast with the BAS, the decomposition of hydroperoxides through chain branching steps (POOH → PO$^\bullet$ + $^\bullet$OH or 2POOH → POO$^\bullet$ + PO$^\bullet$ + H_2O) does not seem to be a viable kinetic path, although commonly invoked as a source of alkoxy macroradicals.[32] Indeed, our calculations (already partly included our study of hydroperoxide formation and decomposition[10]) showed high activation energies; (i) POOH → PO$^\bullet$ + $^\bullet$OH: 2.09 (molecular model) and 2.05 eV (lamellae surface) and (ii) 2POOH → POO$^\bullet$ + PO$^\bullet$ + H_2O: 1.54 (crystalline lamellae) and 0.91 eV (lamellae surface). These reaction pathways can hardly explain not only the decomposition of hydroperoxides but also the formation of other radical species such as alkoxy radicals which are considered to be important for the oxidative degradation of PE,[32] although short lived and not detected by electron paramagnetic resonance.[33] Therefore, we consider other possible reaction pathways with alkyl radicals or other defects, as shown in Figure 2. These reactions still rely on the presence of hydroperoxides. The activation energies obtained for the molecular model, inside crystalline lamellae and at the lamellae surface are summarized in Table 1.

Table 1. Summary of Activation Energies and Enthalphies (Expressed in eV) of Reactions in Figure 2, Leading to Alkoxy Radical Outcomes from Hydroperoxide Decomposition

	activation energy (E_a) [eV]			enthalpy [eV]		
reaction	molecule	crystal	surface	molecule	crystal	surface
1a	1.13	0.51	0.46	−2.11	−2.48	−1.34
2a		0.11	0.62		−2.29	−2.04
3a	1.01	1.29	1.13	0.15	0.93	0.28
4a		1.54	0.91		0.93	0.17
5a		1.51	1.46		1.39	1.07

Overall activation energies are high, with only the first two reactions (1a and 2a), showing a moderate activation energy and a sizeable enthalpy gain. Even these two reactions, however, are of limited relevance at room temperature, if we except the case of the very low barrier (0.11 eV) for reaction 2a in a crystalline environment, whose dependence on oxygen diffusion inside the crystallites will be discussed below. This means that the decomposition of hydroperoxide does not occur easily, and we should look for further alternative pathways to account for the formation of radical species.

On the other hand, the difference in activation energies between reactions occurring inside a crystalline lamella or at its surface, up to 0.5−0.6 eV for reactions 2a and 4a, cannot be ignored, suggesting that when discussing kinetic pathways, it is necessary to take into account the role of the local environment.

As mentioned, reaction 2a has a very small barrier in the crystalline environment; however, its relevance depends on the presence of hydroperoxides inside crystalline lamellae, which is very unlikely if they stem from diffusion of oxygen molecules and formation of peroxy radicals because oxygen diffusion is usually considered to occur essentially in the amorphous region.[8]

However, diffusion in PE is a complex process even simply in the amorphous regions,[34] and we think that if one wants to address the question of the influence of the local environment on the kinetics of PE degradation, one should have a quantitative understanding of the variability of solution energies and energy barriers for diffusion. We previously highlighted the fact that what hinders diffusion inside crystalline lamellae is mainly the

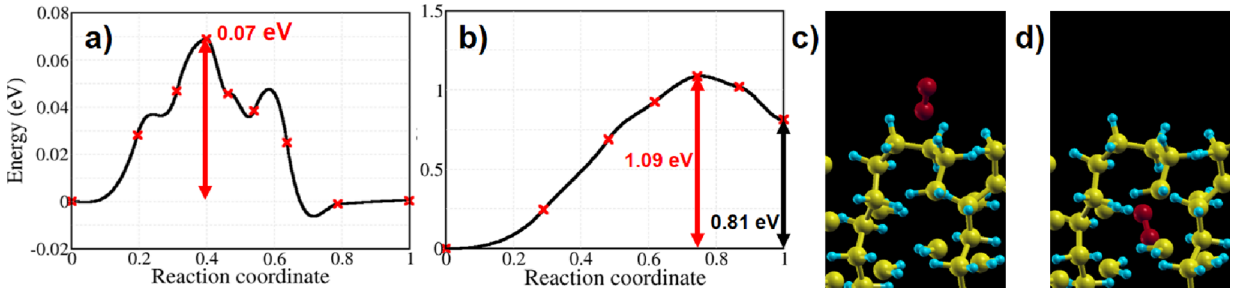

Figure 3. Calculated activation energies and initial and final configurations for the mechanism of oxygen permeation through crystalline lamellae. (a) Energy profile for diffusion of oxygen inside crystalline lamellae, (b) Energy profile for oxygen permeation from the amorphous phase into the crystalline lamellae, (c) oxygen between two lamella surfaces, and (d) oxygen inside a crystalline lamella. Further information on the path is provided in the Supporting Information.

solution energy which is relatively high (on the order of 0.8−1 eV[10]), and we confirm here by further NEB calculations that the migration barrier inside the crystal is indeed quite low (0.07 eV, see Figure 3a).

To gain further insights into the details of oxygen diffusion in PE, we investigated a mechanism which is rarely considered, that is, the permeation of an oxygen molecule from the amorphous phase (Figure 3c) into the crystalline lamellae (Figure 3d); for such a diffusion pathway, we found an energy barrier of 1.09 eV (Figure 3b) which clearly hinders the oxygen diffusion in the crystalline regions. However, we have to note that our amorphous/crystalline interface model is a highly simplified one, with no roughness, no variation in the bent chain distance, and other possible microstructural features. As a further information and for comparison with the mentioned solution energy inside crystalline lamellae, we calculated the solution energy of oxygen between lamellae and found 0.23 eV for our model, where the distance between the lamellae is 1.21 nm, which is in line with at least some reported experimental values.[34]

Given the fact that the formation of alkoxy radicals through hydroperoxide decomposition is not particularly favorable, at least at room temperature, we consider now another reaction for the formation of radical species: it is the reaction from two peroxy radicals ($2POO^{\bullet} \rightarrow [PO^{\bullet} + {}^{\bullet}OP]_{cage} + O_2$), also shown in Figure 4; this constitutes an alternative pathway for the elimination of peroxy radicals, in competition with the one involving hydroperoxide formation and decomposition (see Figure 1).

A recent work featuring a kinetic model based on ab initio results for molecules[19] stresses the importance of this pathway, and also previous studies have shown that taking into account reaction 1b is important for reproducing experimentally some observed autoacceleration effects in the oxidation process. In particular, this reaction was introduced in kinetic models of

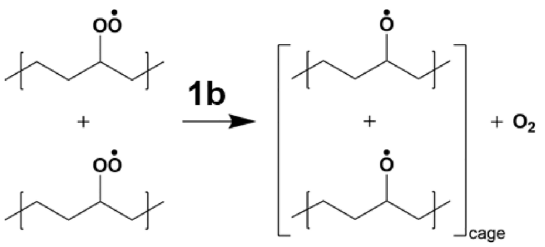

Figure 4. Graphical representation of a bimolecular reaction leading to the formation of alkoxy radicals from two adjacent peroxy ones.

radio-oxidation in order to correctly predict the radio-chemical yields of oxidation products and chain scission[35] and to account for the non-Arrhenius behavior of the oxidation induction time and of the oxidation rate.[36]

For this reaction, as we need the presence of two neighboring peroxy radicals, we considered a few different starting configurations, to determine the cage effect associated to it. The results are summarized in Table 2. They show very different activation energies depending on the environment. The reaction can hardly occur inside crystalline lamellae, whereas there is no barrier on the surface of a lamella. Once peroxy radicals are available—we remind that they are spontaneously formed by oxygen molecules encountering alkyl radicals created under irradiation—alkoxy radicals could be very easily formed by two peroxy radicals. This is in contrast to the production of radical species through decomposition of hydroperoxides, which needs high activation energy. However, reaction 1b needs two localized peroxy radicals, which means that the reaction requires either high concentration of oxygen or low radical diffusion barrier (which is in general excluded for peroxy radicals[32]).

Table 2. Summary of Activation Energies and Enthalpies (Expressed in eV) of the Bimolecular Reaction Depicted in Figure 4, Describing the Formation of Alkoxy Radicals Directly from Peroxy Ones[a]

	activation energy (E_a) [eV]		enthalpy [eV]	
reaction	crystal	surface	crystal	surface
1b	1.30	0.00 (H1)	0.90	−0.27
		0.00 (H2)		−0.27
		0.05 (H3)		−0.09
		0.00 (H4)		−0.32

[a]The role of the environment is highlighted through four different starting configurations (H1−H4) on a lamella surface, and the reaction starting from two neighboring peroxy radicals in a crystalline environment.

The fact that, however, various configurations on the lamellae surface lead to formation of alkoxy radicals without any energy barrier (see Figure 5 for the configurations) suggests that there is probably no entropic barrier either and that the process is essentially limited by oxygen diffusion and the availability of alkyl radicals.

In the following section, we will deal with further reaction pathways, such as crosslinking, chain scission, and the formation carbonyl defects, and how they might be influenced by the local environment.

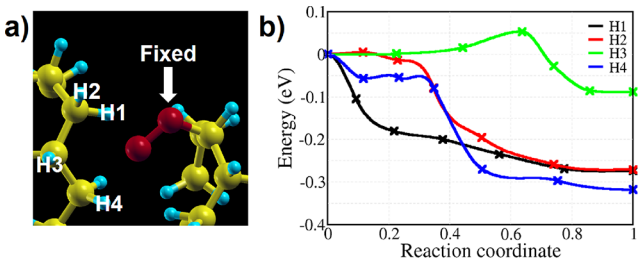

Figure 5. (a) Starting configuration of reaction labeled 1b, where the double bond of a peroxy radical is cleaved to give rise to an alkoxy radical. Here, the reaction takes place at the lamellae surface. H1 to H4 indicate the positions of the second starting peroxy radical (not shown), while the first one (shown and labeled as "fixed") is in the same position for the four considered paths. (b) Energy profiles for reactions with various starting configurations (H1−H4).

Crosslinking Reactions. Several crosslinking reactions take place from radical species; in inert atmosphere, they are expected to be dominant over chain scission,[35] especially through processes involving double bonds.[32] In an oxidation environment, the competition with chain scission will control the chemicrystallization process. Several possible reaction pathways for crosslinking from two radical species are shown in Figure 6.

As all reactions are bimolecular, they cannot then take place on a single chain; we thus omit the molecular model supposed mimicking the low-density regions of the amorphous phase. The results are summarized in Table 3. Of these reactions, three involve alkyl radicals (1c, 2c, and 4c), while the other two (3c and 5c) proceed from alkoxy and peroxy radicals only. We could not find a stable configuration corresponding to reaction 5c at the lamellae surface.

Except for the spatially constrained reaction 1c, the other reactions occur without barriers, meaning that when the concentration of involved radicals is high enough, crosslinking reactions are dominant. And once the reaction takes place, the energy gain is high, so that the product is hardly broken. However, the reactions involving alkyl radicals are, in an oxidizing environment, in competition with the capture of oxygen molecules, to form peroxy radicals, a process that does not need a high concentration of radicals. When the concentration of peroxy radicals is high, the formation of alkoxy radicals would be dominant at the lamellae surface through reaction 1b because reaction 5c does not take place. In contrast to reaction 1b, which as we have shown occurs easily as soon as two peroxy radicals are sufficiently close, crosslinking reactions are, according to our calculations, more sensitive to the starting configuration.

Table 3. Summary of Activation Energies and Reaction Enthalpies (Expressed in eV) for Crosslinking (See Reactions in Figure 6)

	rctivation energy (*Ea*) [eV]		enthalpy [eV]	
reaction	crystal	surface	crystal	surface
1c	0.91	0.55	−0.38	−1.97
2c	0.06	0.00	−1.09	−3.03
3c	0.00	0.00	−1.12	−1.71
4c	0.00	0.00	−2.34	−2.60
5c	0.06	not observed	0.00	not observed

An illustration of this fact is shown in Figure 7, where we propose four variants of reaction 3c, where the initial and final relative position of the alkoxy radicals involved are modified. The four variants are on a lamella surface; two further cases in the crystalline environment (not shown in the figure) show similar behaviors, but the energy barriers are vanishing for three of the six reactions, while others have barriers up to almost 0.4 eV. The fact that some of these reactions present a non-negligible barrier leads to a competition between crosslinking and either β-scission reactions, which will be discussed in the next section, or other reactions leading to ketones.

Chain-Scission Reactions. Carbon−carbon bond scission in pure PE implies large energy barriers or strains,[37] while the nearby presence of radicals can ease the process.[18] A general chain-scission reaction, β-scission, is graphically shown in Figure 8; in these reactions, an alkoxy radical on the chain is decomposed into a primary alkyl radical and an aldehyde. The activation energy of the reaction was calculated for each environment. In the case of crystalline lamellae, the reaction turns out to be unfavorable because we could not find a stable final state with a broken chain: the decomposed chain is spontaneously restored by surrounding chains when the system is relaxed. For the molecular model, different chain lengths are considered, from C_4H_9O to $C_{12}H_{25}O$. The results are summarized in Table 4. In contrast with the molecular model,

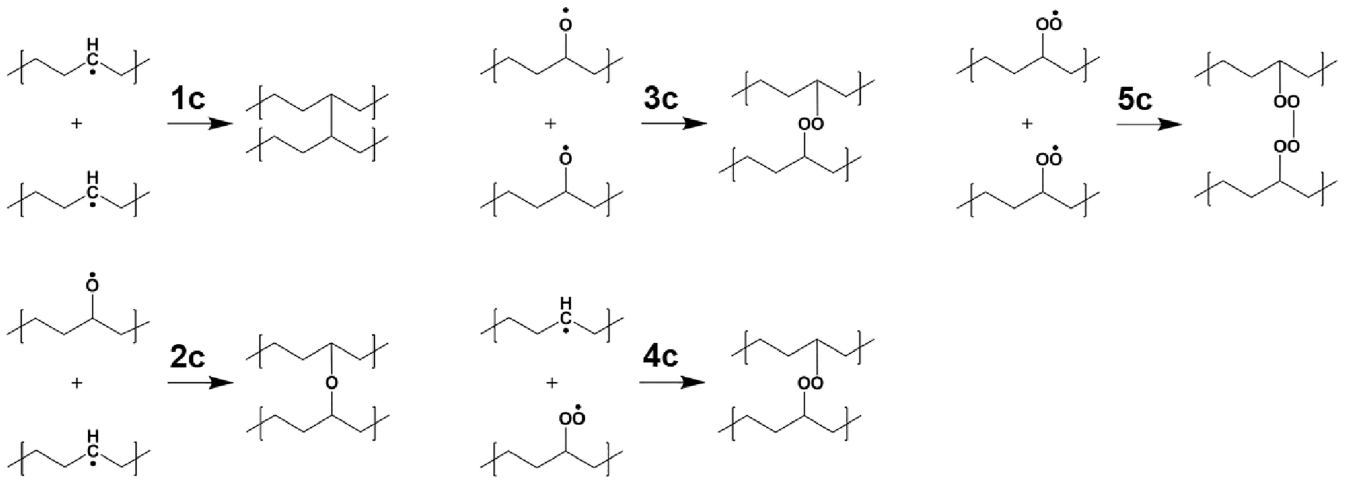

Figure 6. Graphical representation of reactions where two radicals lead to crosslinking.

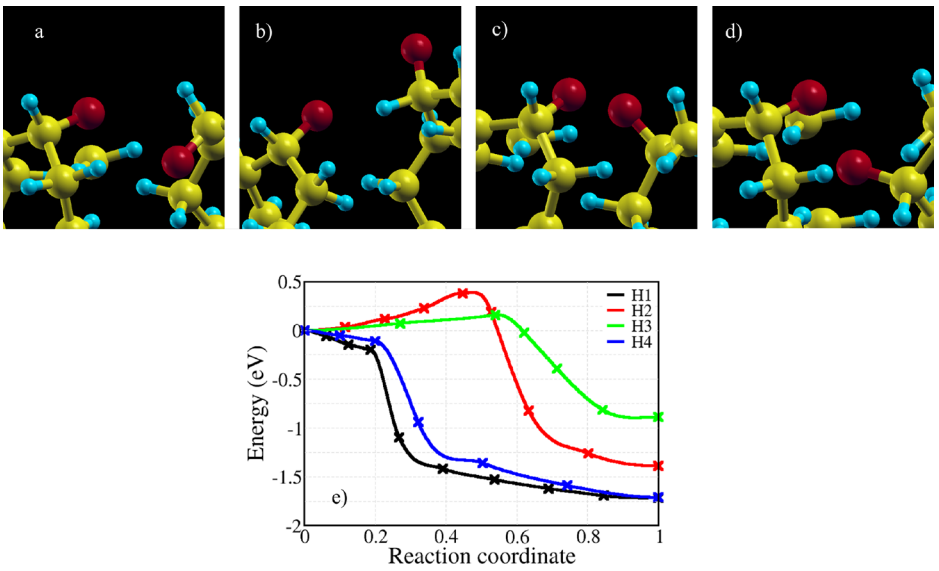

Figure 7. Illustration of four initial alternative initial configurations for reaction 3c (see Figure 6) on a lamella surface (panels a–d), and the corresponding energy profiles for the reactions leading to a peroxy crosslink (panel e). H1–H4 label the four starting positions of one of the alkoxy radicals, the other one being located in the same position for the four configurations.

Figure 8. Graphical illustration of a β-scission reaction starting from an alkoxy radical and giving rise to an aldehyde and a primary alkyl radical.

Table 4. Summary of Activation Energies and Reaction Enthalphies (Expressed in eV) for the β-Scission Reaction Shown in Figure 8[a]

	activation energy (E_a) [eV]		enthalpy [eV]	
reaction	molecule	surface	molecule	surface
1d	0.39 (C_4H_9O)	0.36	0.28	−0.24
	0.44 ($C_8H_{17}O$)		0.36	
	0.42 ($C_{12}H_{25}O$)		0.35	

[a]These reactions can take place at the surface of a PE crystalline lamella but not inside it (the final state is unstable).

β-scission at the crystalline lamellae surface showed a lower activation energy and exothermic reaction, resulting in a more stable final state. This clearly shows that the crystallinity ratio and the details of the microstructure of PE can play a role in determining the rate of chain-scission reactions. We note that the activation energy, 0.3–0.4 eV, is similar to the barriers found for some of the crosslinking reactions, supporting the possibility of a competition between crosslink and chain-scission in oxidizing conditions, with the difference that while crosslinking can occur both in the crystal and at the amorphous or amorphous/crystalline interface, the chain-scission reaction cannot occur inside crystalline lamellae.

Termination through Alcohol and Ketone Groups. Other defects such as alcohols and ketones could be formed by radical species. In particular, ketones are the main products of thermal/photo-degradation. It is therefore important to compare the activation energies between the formation of ketones and/or alcohols and the other reactions discussed in the previous sections. Possible reaction pathways from radical species, leading to ketones and/or alcohols, are summarized in Figure 9. The activation energies for the molecular model, the crystalline lamellae, and at the lamellae surface are summarized in Table 5.

Similar to the formation of a hydroperoxide in unimolecular reactions (H abstraction reactions), alcohol formation tends to have a lower activation energy when the hydrogen atom is not

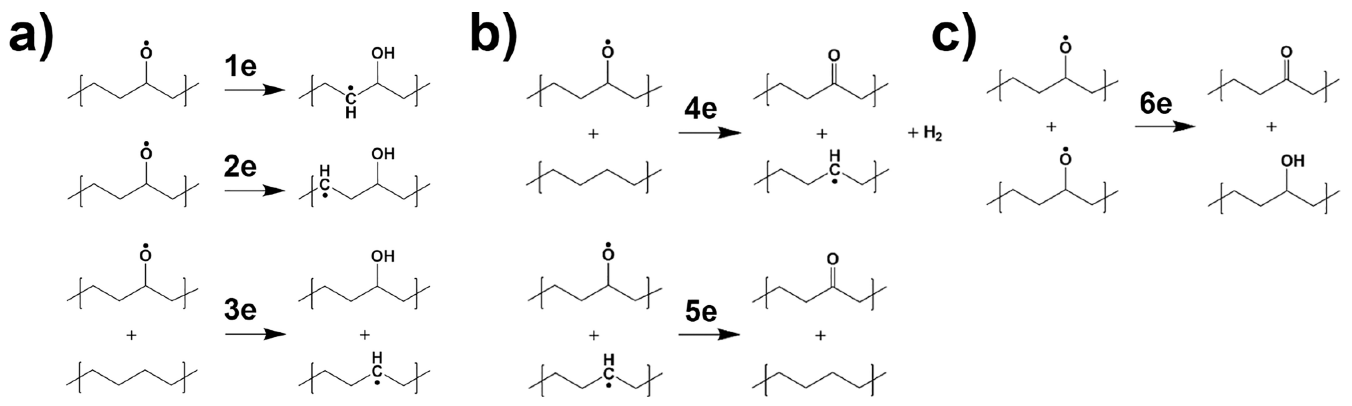

Figure 9. Graphical representation of reactions involving alkoxy radicals in the initial state and leading to ketones and/or alcohols.

Table 5. Summary of Activation Energies and Enthalpies (Expressed in eV) for Reactions Shown in Figure 9, Where Alkoxy Radicals Give Rise to Ketones and Alcohols

	activation energy (E_a) [eV]			enthalpy [eV]		
reaction	molecule	crystal	surface	molecule	crystal	surface
1e	0.93	1.22	0.96	−0.30	−0.11	−0.41
2e	0.53	0.76	0.60	−0.34	−0.16	−0.28
3e		0.74	0.49		−0.20	−0.29
4e		1.04	1.04		0.82	0.23
5e		0.38	0.02		−3.39	−3.18
6e		0.34	0.00		−3.64	−3.66

adjacent to the starting alkoxy radical (reaction 2e is more favorable than 1e). Analogously, the corresponding bimolecular reaction (3e) exhibits lower activation energy than 1e. In the presence of the adjacent alkyl radicals for the formation of ketones, hydrogen atoms are easily detached (5e), especially at the lamella surface where the reaction is barrierless. This is also observed in reaction 6e when a hydrogen transfer occurs between two carbons bearing an alkoxy radical each. Reaction 5e and 6e are definitely the most easy pathways to the formation of ketones and alcohols at the interface between amorphous and crystalline regions, provided alkoxy radicals are available.

DISCUSSION

In the previous sections, we presented the results of calculated barriers for several reactions illustrating the scheme presented in Figure 1. In light of these results, let us recapitulate what are the bottlenecks for the radio-oxidation of PE:

1. oxygen diffusion: the formation of peroxy radicals from O_2 and alkyl radicals is spontaneous, but the diffusion of radicals is slow,[10] and the diffusion of O_2 occurs essentially in the regions between crystalline lamellae but is indeed a bottleneck for reactions to occur inside the crystalline regions.
2. the formation of hydroperoxides is not so easy: barriers in the order of 0.6−0.7 eV have been estimated (except in the case where antioxidants are present).
3. once hydroperoxides are formed, their decomposition, expected to give rise to alkoxy and hydroxyl radicals, is not as easy at room temperature, with energy barriers on the order of 0.4−0.5 eV in the best cases at the lamella surface, if we exclude the possibility of it occurring in the crystal, hindered by oxygen diffusion.
4. an alternative way to form alkoxy radicals through a bimolecular reaction involving two peroxy radicals has very low or null activation energy. Here, the bottleneck stems from the concentration of peroxy radicals, which has to be high enough to provide pairs of radicals sufficiently close to react.

After either bottlenecks 1−3 or 1 and 4 are overcome, the following steps can be quite easily realized; some of these steps take place essentially on the surface of a lamella featuring bent polymer chains, like those in our model of the interface between two lamellae. The mentioned following steps are:

- crosslinking reactions: most of those studied in this paper are spontaneous when the involved species are close enough (i.e., when their concentration is large enough, if we assume that their diffusion is slow). They are strongly exothermic.
- β-scissions: according to our calculations, they are a bit more easily realized on the lamellae surface, but still, there is a barrier of 0.3−0.4 eV to overcome; they are only weakly exothermic.
- formation of ketones and alcohols: two of these reactions are almost spontaneous on the surface and strongly exothermic. They need sufficient concentration of alkoxy and alkyl radicals.

The ratio of alcohols to ketones should be lower than 1 and should approach unity when the concentration of alkoxy radicals is much higher than that of alkyl radicals because in this case, reaction 6e would prevail on 5e, and the former has equal production of ketones and alcohols. Concerning the competition of crosslinking versus chain scission, the latter has a higher activation energy, but it does not need a high concentration of radicals because it is unimolecular, so that in those radio-oxidation stages in which the concentration of alkoxy radicals is not high enough to lead to crosslinking and formation of ketones and alcohols, the fate of isolated alkoxy radicals can be a β-scission reaction. When could this situation be realized? One possibility is that, in samples where hydroperoxides are present before irradiation or when their formation is eased by the presence of phenolic antioxidants, their decomposition through reaction 1a or 2a could lead to isolated alkoxy radicals.

A more thorough assessment of the consequences of the results presented here would stem from using these data on activation energies and reaction enthalpies in a kinetic model based on homogeneous rate theory, that is, following the evolution of the average concentration of each species, or, even better, in an improved kinetic model taking into account at least in a coarse-grained approach, the diverse environments constituting a semicrystalline polymer like PE. Even without going toward object Monte Carlo simulations, which could take into account in detail the heterogeneity of energy deposition and kinetic evolution,[38] a semi-homogeneous rate theory model including similar reactions occurring in low density amorphous regions, at lamellae surfaces and, when possible, inside the lamellae, would allow further insights into polymer degradation kinetics.

SUMMARY AND CONCLUSIONS

In this study, we revisited a subset of reactions that are supposed to contribute to degradation pathways of polyolefins and, in particular, PE through radio-oxidation. The focus is on reactions involving alkoxy radicals, their production inside the polymer, and their fate after further reactions toward stable products. Exploring the energy landscape with the NEB method, we considered the influence of the local environment through three different atomistic models, to understand how reaction barriers may vary with the underlying microstructure.

Reaction pathways toward final products were classified into crosslinking, chain scissions, and other defects (ketones and alcohols).

We globally found that the production of alkoxy radicals is easier through bimolecular peroxy−peroxy radical reactions than by decomposition of hydroperoxides, provided that the concentration of peroxy radicals is high enough. Alkoxy radicals may spontaneously induce crosslinking and also produce ketones and alcohols, again provided their concentration is such that bimolecular reactions between them and other radicals can take place. Otherwise, they can alone lead to β-scissions with activation energies around 0.3−0.4 eV.

For most of the investigated reactions, the local environment proves to be important, with energy barriers lower on lamellae surfaces featuring bent chains than on isolated chains or inside the crystal, as a general trend. Comparing energy barriers and reaction enthalpies, for all calculated reactions, we stress, if it were necessary, the fact that even strongly exothermic reactions can nevertheless be hindered by large energy barriers.

Given the role of alkoxy radicals and their easy formation through bimolecular peroxy−peroxy radical reactions, to prevent oxidation of the polymer scavenging peroxy radicals could be a good strategy; this could be one of the ways phenolic antioxidants act by deactivating peroxy radicals through easier formation of hydroperoxides by H-transfer.

In order to accurately compare the H-transfer reactions involving antioxidants to other degradation reactions, calculations of the activation energies at the atomic scale, with a similar approach to the one presented here, should be the subject of future work.

AUTHOR INFORMATION

Corresponding Author

Guido Roma − *CEA, Service de Recherches de Métallurgie Physique, Université Paris-Saclay, 91191 Gif sur Yvette, France;* orcid.org/0000-0002-9779-4868; Email: guido.roma@cea.fr

Authors

Yunho Ahn − *CEA, Service de Recherches de Métallurgie Physique, Université Paris-Saclay, 91191 Gif sur Yvette, France*

Xavier Colin − *PIMM, Arts et Metiers Institute of Technology, CNRS, CNAM, HESAM University, 75013 Paris, France;* orcid.org/0000-0001-7768-9000

Notes

The authors declare no competing financial interest.

ACKNOWLEDGMENTS

This work was granted access to the HPC resources of TGCC and CINES under the allocation 22010 and 2020-A0090906018 made by GENCI. The project leading to the work presented here has received funding from the Euratom research and training programme 2014−2018 under grant agreement no. 755183. The views expressed here are the responsibility of the author(s) only. The EU Commission takes no responsibility for any use made of the information set out.

REFERENCES

(1) Ferry, M.; Roma, G.; Cochin, F.; Esnouf, S.; Dauvois, V.; Nizeyimana, F.; Gervais, B.; Ngono-Ravache, Y. In *Comprehensive Nuclear Materials*, 2nd ed.; Konings, R. J., Stoller, R. E., Eds.; Elsevier: Oxford, 2020; pp 545−580.

(2) Bolland, J. L.; Gee, G. Kinetic studies in the chemistry of rubber and related materials. II. The kinetics of oxidation of unconjugated olefins. *Trans. Faraday Soc.* **1946**, *42*, 236−243.

(3) Baum, B. The mechanism of polyethylene oxidation. *J. Appl. Polym. Sci.* **1959**, *2*, 281−288.

(4) Ingold, K. U. Inhibition of the Autoxidation of Organic Substances in the Liquid Phase. *Chem. Rev.* **1961**, *61*, 563.

(5) Colin, X.; Richaud, E.; Verdu, J.; Monchy-Leroy, C. Kinetic modelling of radiochemical ageing of ethylene-propylene copolymers. *Radiat. Phys. Chem.* **2010**, *79*, 365−370.

(6) Da Cruz, M.; Van Schoors, L.; Benzarti, K.; Colin, X. Thermo-oxidative degradation of additive free polyethylene. Part I. Analysis of chemical modifications at molecular and macromolecular scales. *J. Appl. Polym. Sci.* **2016**, *133*, 43287.

(7) Chen, L.; Yamane, S.; Sago, T.; Hagihara, H.; Kutsuna, S.; Uchimaru, T.; Suda, H.; Sato, H.; Mizukado, J. Experimental and modeling approaches for the formation of hydroperoxide during the auto-oxidation of polymers: Thermal-oxidative degradation of polyethylene oxide. *Chem. Phys. Lett.* **2016**, *657*, 83−89.

(8) Michaels, A. S.; Bixler, H. J. Flow of gases through polyethylene. *J. Polym. Sci.* **1961**, *50*, 413−439.

(9) Oluwoye, I.; Altarawneh, M.; Gore, J.; Dlugogorski, B. Z. Oxidation of crystalline polyethylene. *Combust. Flame* **2015**, *162*, 3681−3690.

(10) Ahn, Y.; Colin, X.; Roma, G. Atomic Scale Mechanisms Controlling the Oxidation of Polyethylene: A First Principles Study. *Polymers* **2021**, *13*, 2143.

(11) Gryn'ova, G.; Hodgson, J. L.; Coote, M. L. Revising the mechanism of polymer autooxidation. *Org. Biomol. Chem.* **2011**, *9*, 480−490.

(12) Chen, L.; Kutsuna, S.; Yamane, S.; Mizukado, J. ESR spin trapping determination of the hydroperoxide concentration in polyethylene oxide (PEO) in aqueous solution. *Polym. Degrad. Stab.* **2017**, *139*, 89−96.

(13) Gugumus, F. Physico-chemical aspects of polyethylene processing in an open mixer6. Discussion of hydroperoxide formation and decomposition. *Polym. Degrad. Stab.* **2000**, *68*, 337−352.

(14) Henry, J. L.; Ruaya, A. L.; Garton, A. The kinetics of polyolefin oxidation in aqueous media. *J. Polym. Sci., Part A: Polym. Chem.* **1992**, *30*, 1693−1703.

(15) Gijsman, P.; Hennekens, J.; Vincent, J. The mechanism of the low-temperature oxidation of polypropylene. *Polym. Degrad. Stab.* **1993**, *42*, 95−105.

(16) Fayolle, B.; Verdu, J.; Bastard, M.; Piccoz, D. Thermooxidative ageing of polyoxymethylene, part 1: Chemical aspects. *J. Appl. Polym. Sci.* **2008**, *107*, 1783−1792.

(17) Simmie, J. M.; Black, G.; Curran, H. J.; Hinde, J. P. Enthalpies of Formation and Bond Dissociation Energies of Lower Alkyl Hydroperoxides and Related Hydroperoxy and Alkoxy Radicals. *J. Phys. Chem. A* **2008**, *112*, 5010−5016.

(18) de Sainte Claire, P. Degradation of PEO in the Solid State: A Theoretical Kinetic Model. *Macromol* **2009**, *42*, 3469−3482.

(19) De Keer, L.; Van Steenberge, P.; Reyniers, M.-F.; Gryn'ova, G.; Aitken, H. M.; Coote, M. L. New mechanism for autoxidation of polyolefins: kinetic Monte Carlo modelling of the role of short-chain branches, molecular oxygen and unsaturated moieties. *Polym. Chem.* **2022**, *13*, 3304.

(20) Pfaendtner, J.; Yu, X.; Broadbelt, L. J. Quantum Chemical Investigation of Low-Temperature Intramolecular Hydrogen Transfer Reactions of Hydrocarbons. *J. Phys. Chem. A* **2006**, *110*, 10863−10871.

(21) Hayes, C. J.; Burgess, D. R. Kinetic Barriers of H-Atom Transfer Reactions in Alkyl, Allylic, and Oxoallylic Radicals as Calculated by Composite Ab Initio Methods. *J. Phys. Chem. A* **2009**, *113*, 2473−2482.

(22) Kysel, O.; Budzák, Š.; Medved, M.; Mach, P. A DFT study of H-isomerisation in alkoxy-, alkylperoxy- and alkyl radicals: Some implications for radical chain reactions in polymer systems. *Polym. Degrad. Stab.* **2011**, *96*, 660−669.

(23) Xu, A.; Roland, S.; Colin, X. Thermal ageing of a silane-crosslinked polyethylene stabilised with an excess of Irganox 1076. *Polym. Degrad. Stab.* **2021**, *189*, 109597.
(24) Zhou, H.; Wilkes, G. Comparison of lamellar thickness and its distribution determined from d.s.c., SAXS, TEM and AFM for high-density polyethylene films having a stacked lamellar morphology. *Polymer* **1997**, *38*, 5735−5747.
(25) Savage, R. C.; Mullin, N.; Hobbs, J. K. Molecular Conformation at the Crystal-Amorphous Interface in Polyethylene. *Macromol* **2015**, *48*, 6160−6165.
(26) Henkelman, G.; Uberuaga, B. P.; Jónsson, H. A climbing image nudged elastic band method for finding saddle points and minimum energy paths. *J. Chem. Phys.* **2000**, *113*, 9901−9904.
(27) Giannozzi, P.; et al. QUANTUM ESPRESSO: a modular and open-source software project for quantum simulations of materials. *J. Phys.: Condens. Matter* **2009**, *21*, 395502.
(28) Roma, G.; Bruneval, F.; Martin-Samos, L. Optical Properties of Saturated and Unsaturated Carbonyl Defects in Polyethylene. *J. Phys. Chem. B* **2018**, *122*, 2023−2030.
(29) Weber, C. H. M.; Chiche, A.; Krausch, G.; Rosenfeldt, S.; Ballauff, M.; Harnau, L.; Göttker-Schnetmann, I.; Tong, Q.; Mecking, S. Single Lamella Nanoparticles of Polyethylene. *Nano Lett.* **2007**, *7*, 2024−2029.
(30) Ceresoli, D.; Tosatti, E.; Scandolo, S.; Santoro, G.; Serra, S. Trapping of excitons at chemical defects in polyethylene. *J. Chem. Phys.* **2004**, *121*, 6478−6484.
(31) Klimeš, J.; Bowler, D. R.; Michaelides, A. Van der Waals density functionals applied to solids. *Phys. Rev. B: Condens. Matter Mater. Phys.* **2011**, *83*, 195131.
(32) Bracco, P.; Costa, L.; Luda, M. P.; Billingham, N. A review of experimental studies of the role of free-radicals in polyethylene oxidation. *Polym. Degrad. Stab.* **2018**, *155*, 67−83.
(33) Przybytniak, G.; Sadło, J.; Walo, M.; Wróbel, N.; Žák, P. Comparison of radical processes in non-aged and radiation-aged polyethylene unprotected or protected by antioxidants. *Mater. Today Commun.* **2020**, *25*, 101521.
(34) Börjesson, A.; Erdtman, E.; Ahlström, P.; Berlin, M.; Andersson, T.; Bolton, K. Molecular modelling of oxygen and water permeation in polyethylene. *Polymer* **2013**, *54*, 2988−2998.
(35) Khelidj, N.; Colin, X.; Audouin, L.; Verdu, J.; Monchy-Leroy, C.; Prunier, V. Oxidation of polyethylene under irradiation at low temperature and low dose rate. Part I. The case of "pure" radiochemical initiation. *Polym. Degrad. Stab.* **2006**, *91*, 1593−1597.
(36) Khelidj, N.; Colin, X.; Audouin, L.; Verdu, J.; Monchy-Leroy, C.; Prunier, V. Oxidation of polyethylene under irradiation at low temperature and low dose rate. Part II. Low temperature thermal oxidation. *Polym. Degrad. Stab.* **2006**, *91*, 1598.
(37) Hageman, J.; de Wijs, G.; de Groot, R.; Meier, R. Bond scission in a perfect polyethylene chain and the consequences for the ultimate strength. *Macromol* **2000**, *33*, 9098−9108.
(38) Gervais, B.; Ngono, Y.; Balanzat, E. Kinetic Monte Carlo simulation of heterogeneous and homogeneous radio-oxidation of a polymer. *Polym. Degrad. Stab.* **2021**, *185*, 109493.